# Preparation of $Co_{1-z}Al_z(OH)_2(NO_3)_z$ Layered Double Hydroxides and $Li(Co_{1-z}Al_z)O_2$

Wenbin Luo[†,‡] and J. R. Dahn*[,†]

*Department of Physics and Atmospheric Science, Dalhousie University, Halifax B3H3J5, Canada, and School of Metallurgical Science and Engineering, Central South University, Changsha 410083, P.R. China*

*Received June 15, 2008. Revised Manuscript Received October 29, 2008*

The precipitate formed by the addition of an aqueous solution of $Co(NO_3)_2$ and $Al(NO_3)_3$ to LiOH solution has been thoroughly studied as a function of the Al:(Al+Co) ratio, $z$, for $0 \le z \le 1$, using X-ray diffraction and thermogravimetric analysis. For $0 \le z \le 0.2$, the precipitate was a mixed phase of $Co(OH)_2$ and the layered double hydroxide (LDH) $Co_{0.8}Al_{0.2}(OH)_2(NO_3)_{0.2}\cdot nH_2O$. For $0.2 \le z \le 0.4$ the precipitate was a single LDH phase containing both $NO_3^-$ and $CO_3^{2-}$ ions to compensate the $Al^{3+}$ charge. As $z$ increases in this range, the amount of $NO_3^-$ decreases and the amount of $CO_3^{2-}$ increases. For $z > 0.4$, the precipitate was a two phase mixture of an LDH phase and $Al(OH)_3$. $Li[Co_{1-z}Al_z]O_2$ samples were made from the coprecipitated products for $0 \le z \le 0.5$, by calcining the coprecipitate and $Li_2CO_3$. These $Li[Co_{1-z}Al_z]O_2$ samples were compared to samples of the same stoichiometries made by the direct solid state reaction of $Co_3O_4$, $Al(OH)_3$, and $Li_2CO_3$. The lattice constants varied smoothly with $z$ for the $Li[Co_{1-z}Al_z]O_2$ samples made from the coprecipitate. The lattice constants of the solid-state samples deviate from these for $z > 0.15$, suggesting the Al is not uniformly incorporated for $z > 0.15$ in the solid-state samples. The consequences of this are discussed.

## 1. Introduction

Layered double hydroxides (LDHs) have been known for more than 150 years since the discovery of the mineral hydrotalcite.[1−3] They may be generally described by the formula $[M^{2+}{}_{1-z}M^{3+}{}_z(OH)_2][A^{m-}]z/m\cdot nH_2O$, where $M^{3+}$ trivalent metal cations ($Al^{3+}$, $Fe^{3+}$, $Cr^{3+}$, $Ga^{3+}$,$V^{3+}$, etc.) partially substitute for $M^{2+}$divalent metal cations ($Mg^{2+}$, $Ni^{2+}$, $Zn^{2+}$, $Cu^{2+}$, $Fe^{2+}$, etc.) in the brucite-like layers. The positive charge resulting from this substitution is balanced by an exchangeable anion $A^{m-}$($CO_3^{2-}$, $SO_4^{2-}$, $NO_3^-$, $Cl^-$, $Br^-$, etc.) intercalated within the interlayer space. The negatively charged interlayer also can contain some water molecules. Many aspects of layered double hydroxides are well understood, but some detailed aspects of their structure such as the range of possible compositions, the extent of ordering of the metal cations within the layers, the stacking arrangement of the layers, and the arrangement of anions and water molecules in the interlayer galleries are still not fully understood.[4]

Some recent papers describing the composition, structure, and thermal evolution of the structure of LDH compounds are now reviewed. Cavani et al. published a review about the preparation, properties, and applications of hydrotalcite-type anionic clays with the LDH structure.[1] The structure of pillared derivatives of the LDH compounds has been reported.[5] Vaccari reported a comparison of cationic and anionic clays and their physical and chemical properties as well as catalytic applications for the anionic clays.[6] Reichle et al. showed that the heating of Mg−Al LDH materials (to 450 °C) results in the loss of interstitial water, carbon dioxide, and dehydroxylation until a catalytically active material with an approximate composition of $Mg_6Al_2O_8(OH)_2$ remains.[7] Ulibarri et al. observed that Co(II)−A1(III)−$CO_3^{2-}$ hydroxytalcite type materials were not thermally stable to elevated temperatures. During hydrothermal treatment of freshly precipitated $[Co_{1-x}\ Al_x(OH)_2](CO_3)_{x/2}\cdot nH_2O$ materials they found a partial oxidation of Co(II) to Co(III) with simultaneous formation of the $Co_3O_4$ spinel phase.[8]

Due to the possibility of accommodation of different cations in the brucite-like layers, the possibility of intercalation of several types of anions in the interlayer space, and the formation of mixed oxides after thermal treatment, LDHs have been widely studied for catalysis, ion-exchange, adsorption, pharmaceuticals, and photochemistry.[9−15] There have been a few studies of coprecipitated hydroxide intermediates in the production of Li-ion battery positive electrode materials.[16,17] However, studies of LDH intermediate phases used in the production of battery materials are uncommon. We note that Lu et al. reported the synthesis of $Li[Co_x-Mn_{1-x}]O_2$ from a Co−Mn LDH precursor prepared from

* Corresponding author: E-mail: jeff.dahn@dal.ca.
† Dalhousie University.
‡ Central South University.

(1) Cavani, F.; Trifirò, F.; Vaccari, A. *Catal. Today* **1991**, *11*, 173.
(2) Rives,V. *Layered Double Hydroxides: Present and Future*; Nova Science Publishers: New York, 2001.
(3) Khan, A. I.; O'Hare, D. *J. Mater. Chem.* **2002**, *12*, 3191.
(4) Evans, D. G.; Slade, R. C. T.; Duan, X; et al. *Layered Double Hydroxides*; Duan, X., Evans, D. G., Eds.; Structure and Bonding, Vol. 119; Springer-Verlag: Berlin, 2006.
(5) de Roy, A.; Forano, C.; El Malki, K.; Besse, J. P. In *Synthesis of Micrporous Materials*; Ocelli, M. L., Robson, M. E., Eds.; Van Nostrand Reinhold: New York, 1992; Vol. II.
(6) Vaccari, A. *Appl. Clay Sci.* **1999**, *14*, 161.
(7) Reichle, W. T.; Kanf, S. Y.; Everhardt, D. S. *J. Catal.* **1986**, *101*, 352.
(8) Ulibarri, M. A.; Fernández, J. M; Labajos, F. M.; Rives, V. *Chem. Mater.* **1991**, *3*, 626.

10.1021/cm801627t CCC: $40.75 
Published on Web 12/03/2008

mixed nitrate solutions in the presence of air (to make $Mn^{3+}$ and $CO_3^{2-}$).[18]

Now that there is substantial interest in the production of $Li[M_{1-z}Al_z]O_2$ positive electrode materials having Al-substitution within the transition metal, M, layers, it is important to study the impact of Al on the structure and properties of the coprecipitated intermediate. It has been shown that Al-substituted $LiCoO_2$ has a higher average potential versus Li than $LiCoO_2$ and that it has better thermal stability.[19,20] Ohzuku's group showed that Al-substitution in $Li[Ni_{1-z}Al_z]O_2$ reduced the reactivity of the charged electrode material with electrolyte.[21] Since then, Al substitutions have been used to make $Li[Ni_{0.8}Co_{0.15}Al_{0.05}]O_2$ (NCA) and $Li[Ni_{1/3}Mn_{1/3}Co_{1/3-z}Al_z]O_2$ (NMCA)[22] with improved safety compared to the parent materials without Al.

Here, using $Co_{1-z}Al_z(OH)_2(NO_3)_z \cdot nH_2O$ LDH and $Li[Co_{1-z}Al_z]O_2$ as model systems, the composition and structure of the LDH and oxide phases as a function of the Al content, $z$, are studied. The oxides prepared by coprecipitation using the methods described in ref 23 are compared to samples of the same composition made by entirely solid state methods.

## 2. Experimental Section

**2.1. Material Preparation.** *Coprecipitated Layered Double Hydroxide Samples.* A $LiOH \cdot H_2O$ (Sigma Aldrich, 98%) solution and a mixed solution of $Co(NO_3)_2 \cdot 6H_2O$ (Sigma Aldrich, 98%) and $Al(NO_3)_3 \cdot 9H_2O$ (Sigma Aldrich, 98%) were simultaneously added over the course of about 30 min to a stirred flask using a two-channel peristaltic pump (Masterflex C/L pump, Barnant Co.). The concentrations of the solutions were adjusted to set the Al:(Al + Co) ratio, $z$. The precipitate was filtered out and washed with distilled water several times to remove any dissolved salts and then dried at room temperature overnight.

In order to better understand the impact of dissolved $CO_2$ on the composition of the synthesized LDH phases, some coprecipitations were carried out in solutions made with deaerated deionized water (prepared by boiling). These experiments were also made completely under nitrogen to avoid the dissolution of airborne $CO_2$ into the solutions.

*$Li[Co_{1-z}Al_z]O_2$ Samples Prepared by the Coprecipitation Method.* The $Co_{1-z}Al_z(OH)_2(NO_3)_z \cdot nH_2O$ precipitate prepared in air was further dried at 80 °C overnight. The dried precipitate was mixed with an appropriate amount of $Li_2CO_3$ (Alfa Aesar, 99%) and ground. The precursors were heated in air. Samples were heated at 750 °C for 20 h or 900 °C for 3 h.

*$Li[Co_{1-z}Al_z]O_2$ Samples Prepared by the Solid State Method.* Starting materials were $Li_2CO_3$ (Alfa Aesar, 99%), $Co_3O_4$ (Alfa Aesar, 99.7%), and $Al(OH)_3$ (Sigma Aldrich). Stoichiometric amounts of Co- and Al-containing starting materials along with with an appropriate amount $Li_2CO_3$ were mixed and ground together using an automatic grinder (Retsch RM-0). Finally the samples were heated at a certain temperature.

**2.2. Material Characterization.** XRD patterns were collected with a Siemens D5000 diffractometer equipped with a Cu target X-ray tube and a diffracted beam monochromator. LDH samples were measured over a scattering angle range between 2 and 90° using 0.05° steps and a 5 s counting time. $Li[Co_{1-z}Al_z]O_2$ samples were measured over a scattering angle range between 10 and 90° using 0.05° steps and a 10 s counting time.

Thermogravimetric analysis (TGA) was carried out using a TA instruments SDT-Q600 TGA in the temperature range between 25 and 500 °C using a heating rate of 5 °C/min and an air flow rate of 50 mL/min.

Atomic absorption spectroscopy performed at the Minerals Engineering Center at Dalhousie University was used to measure the Al:(Al + Co) ratio in the coprecipitated hydroxide samples prepared in air. CHN analysis was performed on the all the coprecipitated hydroxide samples at Canadian Microanalytical Services in Delta, B.C., Canada.

## 3. Results and Discussion

Figure 1 shows the XRD patterns of the coprecipitates prepared in air for $0 \leq z \leq 1$. The coprecipitate is single phase $Co(OH)_2$ at $z = 0$. The Bragg peaks in Figure 1 for $z = 0$ have been indexed based on the hexagonal structure (space group: $P\bar{3}m1$) of $Co(OH)_2$. For $z = 0.05$, 0.1, and 0.15, the XRD patterns in Figure 1 show the coexistence of two phases, $Co(OH)_2$ and a layered double hydroxide phase. The (001) Bragg peak of $Co(OH)_2$, indicated by a triangle in Figure 1, decreases in intensity as $z$ increases from 0 to 0.2. When $z = 0.2$, there is virtually no $Co(OH)_2$ left in the sample. When $0.2 \leq z \leq 0.4$, the XRD patterns in Figure 1 show the presence of only a single phase. The Bragg peaks of this phase have been indexed for $z = 0.2$ based on the layered double hydroxide structure described by JCPDS File No. 22-700.[24] The stoichiometry of the LDH phase is thought to be $Co_{1-z}Al_z(OH)_2(NO_3)_{0.4-z}(CO_3)_{z-0.2} \cdot nH_2O$ as will be demonstrated later below. The diffraction peaks corresponding to the (003) and (006) planes become weaker and broader as $z$ increases from 0.2 to 0.4.

Figure 2 shows an enlargement of the data from Figure 1 for $0.4 \leq z \leq 0.6$. Two weak peaks corresponding to characteristic peaks of $Al(OH)_3$ appear around $2\theta = 20°$ at $z = 0.5$ in Figure 2. Apparently an Al content beyond $z = 0.4$ cannot be accommodated within the brucite-like layers

(9) Climent, M. J.; Corma, A.; Iborra, S.; Velty, A. *J. Catal.* **2004**, *221*, 474.
(10) Intissar, M.; Jumas, J. C.; Besse, J. P.; Leroux, F. *Chem. Mater.* **2003**, *15*, 4625.
(11) Tsen, W. Y.; Lin, J. T.; Mou, C. Y; Cheng, S. F.; Liu, S. B.; Chu, P. P; Liu, H. W. *J. Am. Chem. Soc.* **1996**, *18*, 4411.
(12) Choy, J. H.; Kwak, S. Y.; Park, J. S.; Jeong, Y. J.; Portier, J. *J. Am. Chem. Soc.* **1999**, *121*, 1399.
(13) Choy, J. H.; Oh, J. M.; Park, M.; Sohn, K. M.; Kim, J. W. *Adv. Mater.* **2004**, *16*, 1181.
(14) Evans, D. G.; Xue, D. A. *Chem. Commun.* **2006**, 485.
(15) Lei, L. X.; Zhang, W. F.; Hu, M.; O'Hare, D. *J. Inorg. Chem.* **2005**, *21*, 451.
(16) Jouanneau, S.; Dahn, J. R. *Chem. Mater.* **2003**, *15*, 495.
(17) Guilmard, M.; Pouillerie, C.; Croguennec, L.; Delmas, C. *Solid State Ionics* **2003**, *160*, 39.
(18) Lu, Y.; Wei, M.; Yang, L.; Li, C. *J. Solid State Chem.* **2007**, *180*, 1775.
(19) Aydinol, M. K.; Kohan, A. K.; Ceder, G; Cho, K.; Joannopoulos, J. *Phys. Rev. B* **1997**, *56*, 1354.
(20) Ceder, G.; Chiang, Y.-M.; Sadoway, D. R.; Aydinol, M. K.; Jang, Y.-I.; Huang, B. *Nature* **1998**, *392*, 694.
(21) Ohzuku, T.; Ueda, A.; Kouguchi, M. *J. Electrochem. Soc.* **1995**, *142*, 4033.
(22) Zhou, F.; Zhao, X. M.; Lu, Z. H.; Jiang, J. W.; Dahn, J. R. *Electrochem. Commun.*, **2008**, *10*, 1168.
(23) Lu, Z. H.; MacNeil, D. D.; Dahn, J. R. *Electrochem. Solid-State Lett.* **2001**, *4* (11), A191–A194.
(24) Joint Commission on Powder Diffraction Standards, International Center for Diffraction Data, 12 Campus Boulevard, Newtown Square, PA, USA, 1907-33273.

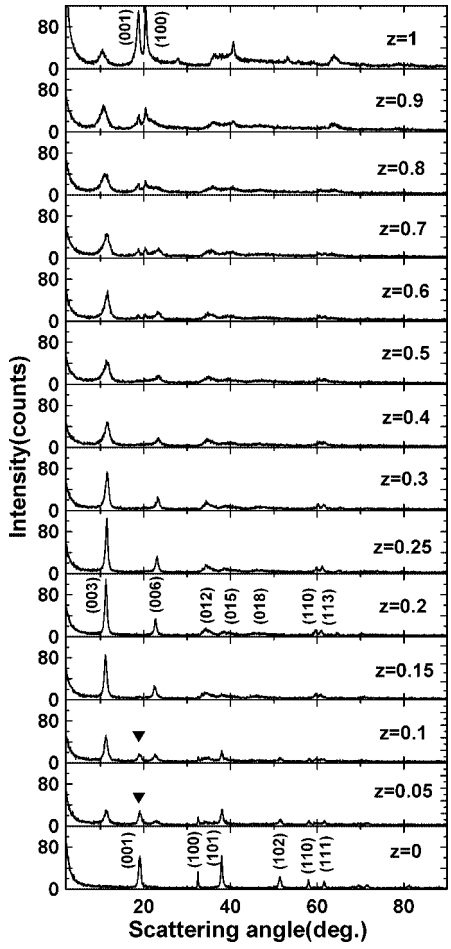


**Figure 1.** XRD patterns of the products of the coprecipitation of $Co(NO_3)_2 \cdot 6H_2O$ and $Al(NO_3)_3 \cdot 9H_2O$ in LiOH solution. The value of the Al:(Al + Co) ratio, $z$, is given next to each pattern. The Miller indices of the Bragg peaks of $Co(OH)_2$ are given near the peaks for $z = 0$. The Miller indices of the layered double hydroxide phase are given next to the Bragg peaks of the sample with $z = 0.2$. Two Bragg peaks are indexed based on the $Al(OH)_3$ structure in the pattern with $z = 1$.

and the excess Al precipitates as $Al(OH)_3$ when $z > 0.4$. The intensity of the (001) and (100) Bragg peaks of $Al(OH)_3$ (indicated for $z = 1$ in Figure 1) increases as $z$ increases for $z > 0.5$.

The XRD pattern for $z = 1$ in Figure 1 shows some characteristic peaks similar to those of the LDH phase in addition to the peaks from $Al(OH)_3$. This sample contains no cobalt atoms. It is possible these peaks originate from a gibbsite-type Li−Al LDH phase. Gibbsite, or $\gamma$-$Al(OH)_3$, takes a layered structure and can simultaneously intercalate cations and anions, for example, as found in $LiAl_2(OH)_6Cl$. Perhaps there is a $NO_3$-containing equivalent of this phase. However, the $NO_3$-content of this phase would have to be very small due to the fact that the weight loss upon heating (to be described later below) is well-explained if the sample is completely $Al(OH)_3$. Further work would be needed to understand the $z = 1$ pattern better.

Figure 3 shows the variation of the lattice constants, $a$ and $c$, of the LDH phase prepared in air for $0.15 \leq z \leq 0.5$. The lattice constant $a$ is the average distance between nearest neighbor metal cations in the same brucite-like layer. The lattice constant $a$ decreases as the Al content, $z$, increases, since the ionic radius of $Al^{3+}$ is smaller than that of $Co^{2+}$

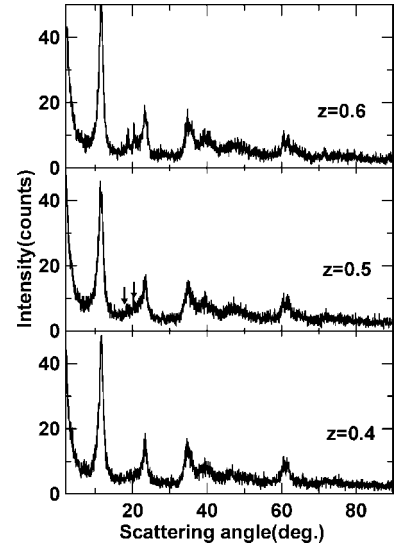


**Figure 2.** Expanded view of the XRD patterns from Figure 1 for samples with $0.4 \leq z \leq 0.6$.

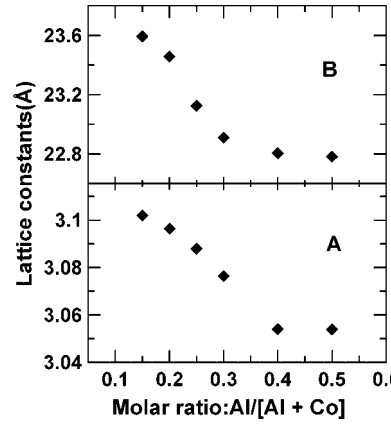


**Figure 3.** Lattice constants $a$ [panel A] and $c$ [panel B] versus $z$, the Al/(Al + Co) ratio.

(0.51 Å vs 0.72 Å).[25] The lattice constant $c$ is three times the spacing between the centers of the brucite-like layers and is determined by the thickness of the brucite-like layer $[Co_{1-z}Al_z(OH)_2]^{z+}$ and the thickness of the anion-filled gallery. The decrease of $c$ with $z$ can be explained by the stronger electrostatic interaction between the positively charged brucite-like layer and the negatively charged anion filled gallery. Figure 3 shows that both $a$ and $c$ remain constant for $z \geq 0.4$, suggesting the composition of the LDH phase does not vary substantially in the two phase LDH−$Al(OH)_3$ region.

Figure 4 shows the variation of the measured Al content in the samples by AA analysis compared to the expected content based on the mole ratios used during synthesis. The agreement is excellent, proving that the aluminum is incorporated within the samples.

Figure 5 shows the results of C and N analysis of the coprecipitated hydroxide samples. Small black data points are for samples synthesized in air and large red data points are for samples synthesized under nitrogen with deaerated water. The N content increases until about $z = 0.16$ consistent

(25) West, R. C.; Lide, D. R.; Astle, M. J.; Beyer W. H. *CRC Handbook of Chemistry and Physics*, 70th ed.; CRC Press: Boca Raton, FL, 1990.

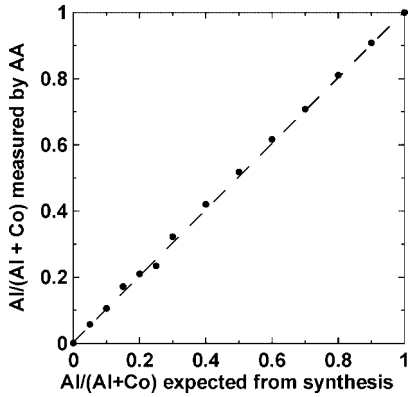


**Figure 4.** Al:(Al + Co) ratio measured by AA analysis plotted versus that expected from synthesis.

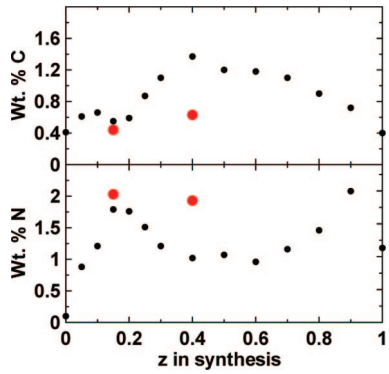


**Figure 5.** Carbon and nitrogen weight percent in coprecipitated samples prepared in air (small symbols) and under anaerobic conditions (large red symbols) plotted versus the aluminum content, $z$.

with the incorporation of $NO_3^-$. Between $0.2 < z < 0.4$ the amount of nitrogen decreases and the amount of carbon increases for the samples synthesized in air. This is consistent with the substitution of $NO_3^-$ by $CO_3^{2-}$ in this composition range in order to accommodate more $Al^{3+}$ in the layers presumably since the number of anions that can pack into the galleries is limited to near 1/6 per metal atom. The sample with $z = 0.15$ made in anaerobic conditions matches the composition of the sample made in air. However, the sample with $z = 0.4$ made in anaerobic conditions has much less carbon than the sample made in air and has the same N content as the $z = 0.15$ sample. This suggests that the exchange of $CO_3^{2-}$ for $NO_3^-$ does not occur under anaerobic conditions, as expected.

Thermogravimetric analysis was used in order to learn more about the intercalated anions present in the galleries of the LDH phase. Since $NO_3$ and $CO_3$ are more massive than OH, the amounts of each anion can be studied by TGA, since all evolve as the samples are heated to 500 °C and are converted to $(Co_{1-z}Al_z)_3O_4$ spinel phases. Figure 6 shows the percent mass versus temperature for the coprecipitated samples prepared in air for $0 \leq z \leq 1$. The TGA curves show that the mass loss occurs in two steps. The first step is believed to be the removal of physisorbed and intercalated water in the range between 25 and 150 °C. The second step between 150 and 500 °C is associated with the loss of $NO_3$, $CO_3$, and OH and the conversion of the sample to the spinel oxide (and $Al_2O_3$ for large $z$). Figure 6 shows that the total mass lost between 25 and 500 °C increases rapidly with $z$

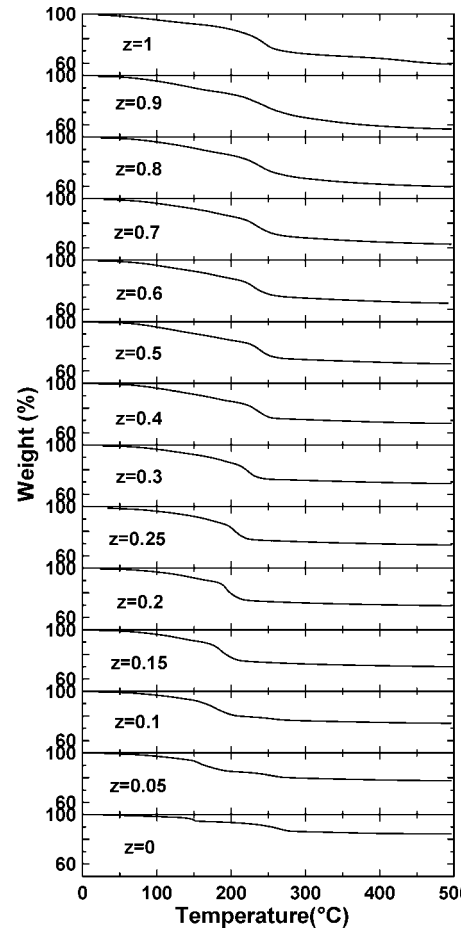


**Figure 6.** Percent retained mass versus temperature for the coprecipitated samples heated in air. The values of the aluminum content, $z$, are given in each panel.

for $0 < z < 0.2$ and then varies slowly with $z$ for $z > 0.2$. This suggests that the amount of $NO_3^-$ anions in the galleries does not increase substantially for $z > 0.2$. Since $CO_3$ and $NO_3$ have almost identical masses, the mass loss remains relatively constant in the range between $0.2 < z < 0.4$, where $CO_3^{2-}$ is observed to replace $NO_3^-$ based on the CHN measurements. This observation will be further discussed later below.

Figure 7 shows the derivative of the mass with respect to temperature plotted versus temperature (the differential thermograms or DTG curves) for all the samples prepared in air. The maximum rate of mass loss is recorded as a peak in the DTG curve. For $0 \leq z \leq 0.2$, two peaks on the DTG curve are observed. The higher temperature peak decreases in intensity with $z$ and is associated with the $Co(OH)_2$ phase. The lower temperature peak in the range $0 \leq z \leq 0.2$ for $z \geq 0.05$ is associated with the LDH phase and increases in intensity with $z$. For $0.2 \leq z \leq 0.4$, the DTG peak shifts to higher temperature with $z$, consistent with varying properties in a single phase region of variable stoichiometry, in agreement with the XRD results presented in Figures 1 and 3 and the CHN testing results presented in Figure 5. The peaks of the DTG curves for $0.4 \leq z \leq 1$ do not change very much. This is consistent with a two phase mixture of an LDH phase and $Al(OH)_3$ in this composition range, provided each phase has approximately the same DTG curve, in agreement with the XRD results presented in Figures 1 and 2.

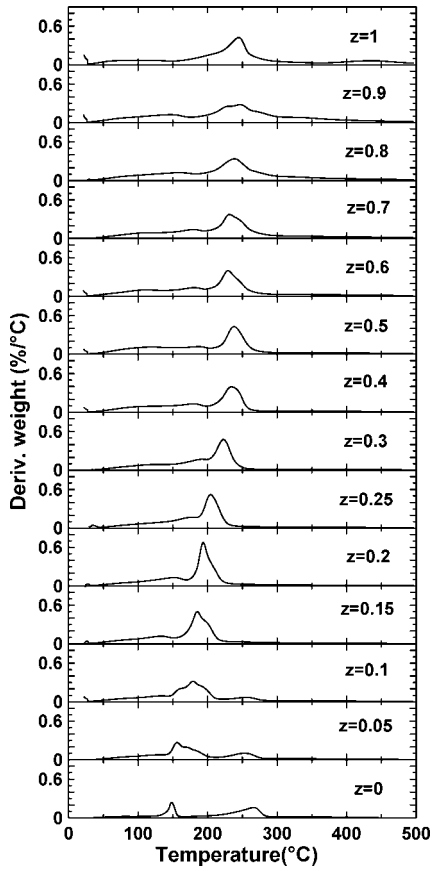


**Figure 7.** DTG patterns for the data in Figure 6.

Figure 8 compares the XRD patterns of samples with $z = 0.15$ and $z = 0.4$ prepared under air and under anaerobic conditions. The $z = 0.15$ patterns are similar with the sample prepared under anaerobic conditions having more $Co(OH)_2$ phase remaining, suggesting $z = 0.15$ is still within the two phase region. We suggest that the 2-phase region ends at $z = 0.2$. The sample with $z = 0.4$ prepared under anaerobic conditions shows clear evidence of the $Al(OH)_3$ phase which did not appear until higher values of $z$ (see Figure 2) for the samples made in air. This suggests the extent of the single phase LDH range is much less when there is no doubly charged anion (e.g., $CO_3^{2-}$) present to compensate the charge of more Al.

Figure 9 shows the XRD patterns of coprecipitated samples (prepared in air) after the TGA test. The diffraction patterns suggest that the spinel series $(Co_{1-z}Al_z)_3O_4$ was obtained, at least over the range $0 \leq z \leq 0.4$. The Bragg peaks of the sample with $z = 0$ have been indexed according to the spinel structure of $Co_3O_4$. All of the patterns for all values of $z$ show the presence of the same set of diffraction peaks, but the full width at half-maximum of the peaks increases as $z$ increases. In addition, the background in the diffraction pattern increases above $z = 0.5$ and is substantial for $z = 0.9$ and $z = 1.0$, suggesting the presence of an amorphous or nanocrystalline phase. Since Al can only exist in oxidation state $3^+$, the maximum value $z$ could take in the $(Co_{1-z}Al_z)_3O_4$ spinel phase is $z = 0.67$. When $z = 1$, we expect the product of heating after TGA to be $Al_2O_3$, which probably accounts for the high background levels if the formed $Al_2O_3$ is amorphous.

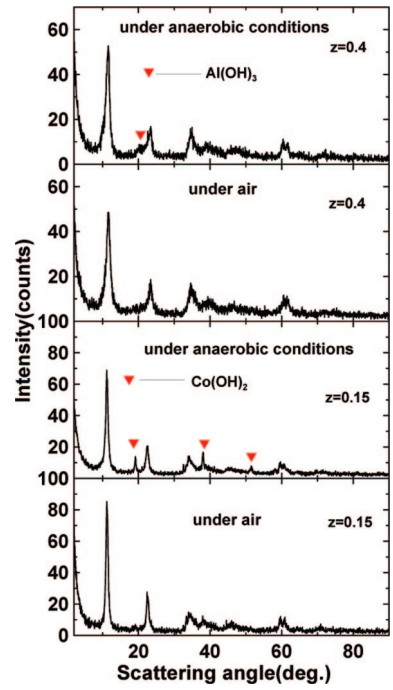


**Figure 8.** XRD patterns of coprecipitated samples with $z = 0.15$ and $z = 0.4$ prepared in air or under anaerobic conditions as indicated. Bragg peaks discussed in the text are highlighted by arrows.

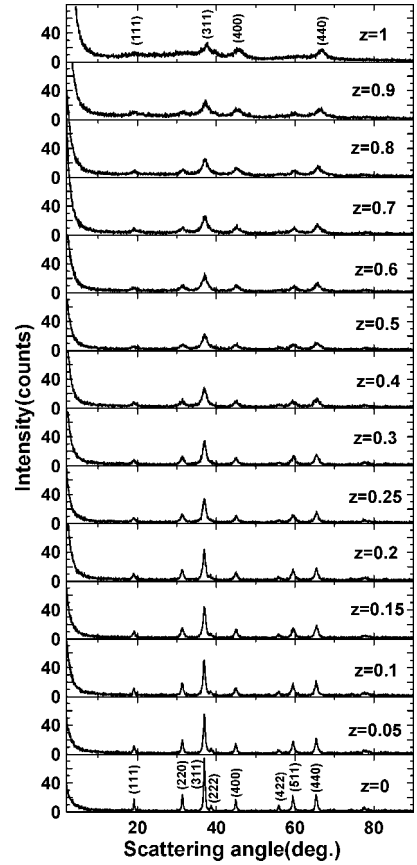


**Figure 9.** XRD patterns of the coprecipitated samples after TGA to 500 °C in air. The Miller indices of $Co_3O_4$ spinel are given next to the Bragg peaks of the $z = 0$ sample.

The interpretation of the X-ray patterns in Figure 9 should be consistent with the phase information extracted from Figures 1−3. For $0 \leq z \leq 0.4$, a mixed $(Co_{1-z}Al_z)_3O_4$ spinel

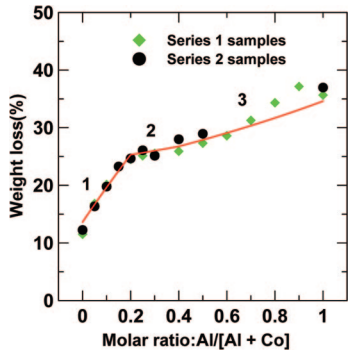


**Figure 10.** Measured % mass loss between 150 and 500 °C for the coprecipitated samples as determined from Figure 4. The solid curve is the calculated weight loss based on the phases present in the coprecipitated samples as described in the text and in Figure 11.

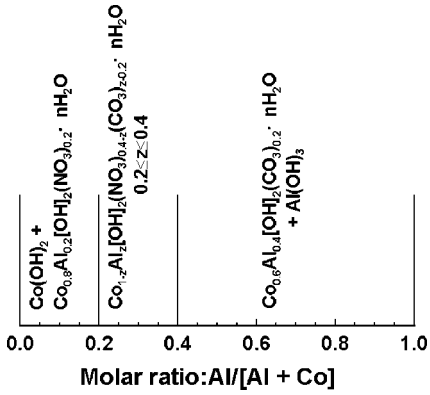


**Figure 11.** Phase diagram showing the phases present in the coprecipitate (prepared in air) as a function of $z$, the Al/(Al + Co) ratio.

phase is expected and is observed in Figure 9. For $z > 0.4$, the precipitate is believed to be a mixture of an LDH phase with $z = 0.4$ and $Al(OH)_3$. The LDH phase should convert to the spinel phase with $z = 0.4$ and $Al(OH)_3$ should convert to $Al_2O_3$. This is consistent with the diffraction patterns in Figure 9, if the increase in background is associated with amorphous or nanocrystalline $Al_2O_3$. The patterns for $z = 0.9$ and $z = 1$ show broad Bragg peaks in about the same positions as the spinel phase, but these must be associated with nanocrystalline $Al_2O_3$. The diffraction angles of the strongest $Al_2O_3$ peaks[26] are almost coincident with the spinel phase peaks and hence are hard to distinguish.

Figure 10 shows the percent mass loss in the region between 150 and 500 °C plotted versus the aluminum content, $z$, for two different batches of samples prepared in air in order to demonstrate the reproducibility of the experiments. The solid curve in Figure 10 is the predicted weight loss based on an interpretation of the experiments in Figures 1−9. For $0 \le z \le 0.2$, the solid line has been calculated assuming the mixed phases of $(0.2 - z)/0.2$ $Co(OH)_2$ and $z/0.2$ $Co_{0.8}Al_{0.2}(OH)_2(NO_3)_{0.2}$ convert to $Co_3O_4$ and $(Co_{0.8}Al_{0.2})_3O_4$, respectively. For $0 \le z \le 0.2$, the solid line matches the data in Figure 10 well.

Figure 10 shows a strong decrease in the rate of weight loss with $z$ at $z = 0.2$, suggesting no further anions are incorporated into the solid for $z > 0.2$. Figures 1 and 3 show a single phase LDH with varying lattice parameters between

(26) Wyckoff, R. W. G. *Crystal structures*, 2nd ed.; Robert E. Kreiger Publishing Company: Malabar, FL, 1981; Vol. 3, p 77.

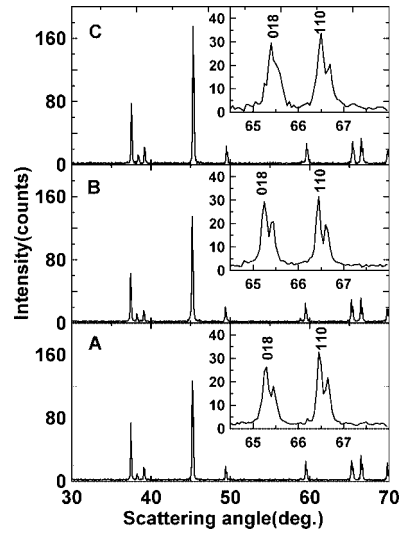


**Figure 12.** XRD patterns of $Li[Co_{0.8}Al_{0.2}]O_2$ synthesized using different methods (A: coprecipitation method, 750 °C, 20 h; B: coprecipitation method, 900 °C, 3 h; C: solid state method, 900 °C, 3 h). The inset graphs show an expanded view of the diffraction patternS near the (018) and (110) peaks.

$0.2 \le z \le 0.4$. The CHN measurements show that $NO_3^-$ is replaced by $CO_3^{2-}$ in this range. The weight loss during TGA, therefore, should be roughly constant over this composition range, as observed. The solid line in Figure 10 for $0.2 \le z \le 0.4$ has been calculated assuming that the single phase is $Co_{1-z}Al_z(OH)_2(NO_3)_{0.4-z}(CO_3)_{z-0.2}$ and that this phase decomposes to $(Co_{1-z}Al_z)_3O_4$ upon heating to 500 °C. The solid line agrees well the data in Figure 10 for $0.2 \le z \le 0.4$.

When $z > 0.4$, the coprecipitate is thought to be a mixed phase of the LDH phase $Co_{0.6}Al_{0.4}(OH)_2(CO_3)_{0.2}$ and $Al(OH)_3$. The solid line for $0.4 \le z \le 1.0$ in Figure 10 was calculated assuming these phases decompose to $(Co_{0.6}Al_{0.4})_3O_4$ and $Al_2O_3$, respectively, consistent with the XRD and DTG results. The solid line in Figure 10 for $0.4 \le z \le 1.0$ fits the experiments well.

Figure 11 shows a phase diagram for the product of the coprecipitation in air. Figure 11 was constructed based on the interpretation of the XRD, CHN, DTG, and TGA weight loss experiments described above.

Figure 12 displays the XRD patterns ($30° < 2\theta < 70°$) of $Li[Co_{0.8}Al_{0.2}]O_2$ prepared by the coprecipitation method (in air) and the solid state method. These data demonstrate that the compounds are single phase. All of peaks can be indexed based on the hexagonal α-$NaFeO_2$ structure (space group: $R\bar{3}m$). The inset graphs in Figure 12 show an expanded view of the (018) and (110) Bragg peaks. The sample prepared by solid state synthesis has the broadest Bragg peaks with poorly resolved $K_\alpha$ doublets. This may indicate a range of Al contents in various particles, because the lattice constants vary with $z$ in $LiCo_{1-z}Al_zO_2$. Figure 13 shows the XRD patterns of $LiCo_{1-z}Al_zO_2$ ($0.3 \le z \le 0.5$) samples prepared by the solid state method. Figure 13 shows the presence of impurity peaks for $z \ge 0.4$, suggesting that all the Al is not incorporated into the layered structure for synthesis by the solid state method when $z > 0.3$.

Figure 14 shows the lattice constants ($a$ and $c$) as a function of $z$ in $LiCo_{1-z}Al_zO_2$ for samples prepared by the

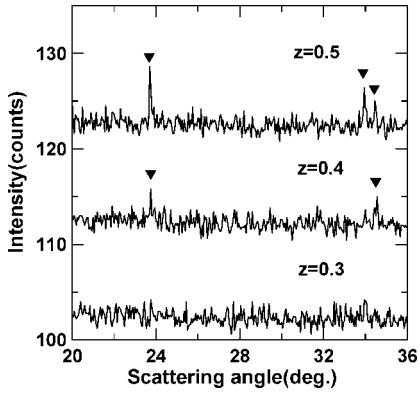


**Figure 13.** Expanded views of portions of XRD patterns of $Li[Co_{1-z}Al_z]O_2$ ($0.3 \leq z \leq 0.5$) synthesized using the solid state method. Impurity peaks are indicated with triangles.

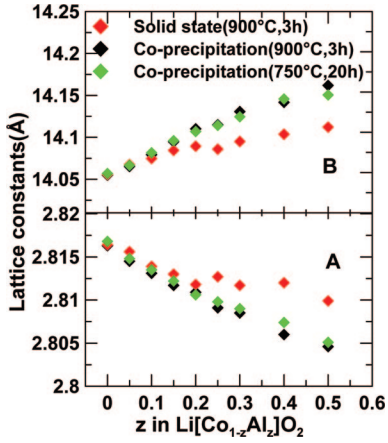


**Figure 14.** Lattice constants, *a* [panel A] and *c* [panel B], of $Li[Co_{1-z}Al_z]O_2$ versus *z*. Data for samples prepared by the coprecipitation method (750 and 900 °C) and by the solid-state method (900 °C) are indicated.

solid state and coprecipitation methods. The lattice constant *a* decreases and *c* increases as *z* increases. The lattice constants vary smoothly with *z* for the coprecipitated samples but deviate for the solid state samples above $z = 0.15$. This suggests that the solid state method may not produce materials with a uniform cation distribution when the aluminum content is large, consistent with the results in Figures 12 and 13. Ticado et al. synthesized the $LiCo_{1-z}Al_zO_2$ solid solution series using a citrate precursor method.[27,28] They found that a solid solution phase with Co and Al atoms randomly occupying octahedral sites extended from $z = 0$ to about $z = 0.9$.

Figure 15 compares our lattice constant results with literature results from other research groups. The literature results selected are all for samples which were not prepared by solid state methods. The excellent agreement between our

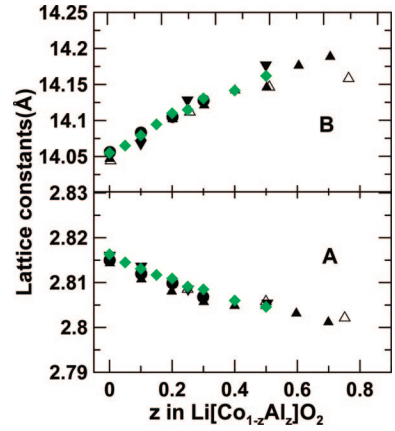


**Figure 15.** Lattice constants, *a* [panel A] and *c* [panel B], versus *z* in $Li[Co_{1-z}Al_z]O_2$. These results (◆) coprecipitation method (900 °C; 3 h) are compared to the results from (▲) ref 29, (●) ref 30, (▼) ref 31, and (△) ref 32.

results and the literature results suggests that the coprecipitation method, even in the presence of the formation of layered double hydroxides as intermediate phases, can be used to produce state-of-the-art $Li(Co_{1-z}Al_z)O_2$ samples.

## 4. Conclusion

The precipitate formed by the addition of an aqueous solution of $Co(NO_3)_2$ and $Al(NO_3)_3$ to LiOH solution in air or under anaerobic conditions has been thoroughly studied as a function of the Al:(Al + Co) ratio, *z*, for $0 \leq z \leq 1$, using X-ray diffraction and thermogravimetric analysis. For $0 \leq z \leq 0.2$, the precipitate was a mixed phase between $Co(OH)_2$ and the layered double hydroxide (LDH) $Co_{0.8}Al_{0.2}(OH)_2(NO_3)_{0.2}\cdot nH_2O$. For $0.2 \leq z \leq 0.4$ the precipitate is a single LDH phase containing both $NO_3^-$ and $CO_3^{2-}$ ions. For $z > 0.4$, the precipitate was a two phase mixture of an LDH phase and $Al(OH)_3$. A phase diagram for the structure and composition of the coprecipitate as a function of aluminum content was determined and is included as Figure 11.

$Li[Co_{1-z}Al_z]O_2$ samples were made from the coprecipitated products for $0 \leq z \leq 0.5$, by calcining the coprecipitate and $Li_2CO_3$. These $Li[Co_{1-z}Al_z]O_2$ samples were compared to samples of the same stoichiometries made by the direct solid state reactions of $Co_3O_4$, $Al(OH)_3$, and $Li_2CO_3$. The lattice constants vary smoothly with *z* for the $Li[Co_{1-z}Al_z]O_2$ samples made from the coprecipitate. The lattice constants of the solid-state samples deviate from these for $z > 0.15$, suggesting the Al is not uniformly incorporated for $z > 0.15$ in the solid-state samples.

Researchers and companies involved in producing Al-substituted layered transition metal oxides as positive electrode materials should be aware that layered double hydroxides form when Al is included in the coprecipitation step. Nitrate-containing LDHs decompose below 500 °C and allow the production of Al-substituted oxides with an apparently homogeneous cation distribution. By contrast, Al-substituted samples prepared using the same heating schedule by solid state methods may not have a homogeneous cation distribution.

**Acknowledgment.** The authors thank NSERC and 3M Canada for funding this work under the auspices of the Industrial Research Chair program. W.L. thanks the China Scholarship Council for scholarship support.

CM801627T

(27) Alcántara, R.; Lavela, P.; Relano, P. L.; Tirado, J. L.; Zhecheva, E.; Stoyanova, R. *Inorg. Chem.* **1998**, *37*, 264.
(28) Gaudin, E.; Taulelle, F.; Stoyanova, R.; Zhecheva, E; Alcantara, R.; Lavela, P.; Tirado, J. L. *J. Phys. Chem. B* **2001**, *105*, 8081.
(29) Khan, M. N.; Bashir, J. *Mater. Res. Bull.* **2006**, *41*, 1589.
(30) Myung, S. T.; Kumagai, N.; Komaba, S.; Chung, H. T. *Solid State Ionics* **2001**, *139*, 47.
(31) Yoon, W. S.; Lee, K. K.; Kim, K. B. *J. Electrochem. Soc.* **2000**, *147*, 2023.
(32) Yang, Y. I.; Huang, B. Y.; Wang, H. F.; Sadoway, D. R.; Ceder, G.; Chiang, Y. M.; Liu, H.; Tamura, H. *J. Electrochem. Soc.* **1999**, *146*, 862.